




Repeatability of Peripapillary Optical Coherence Tomography Angiography Parameters in Older Adults

Cason B. Robbins, BS¹ , Dilraj S. Grewal, MD¹,
Atalie C. Thompson, MD, MPH¹, Stephen P. Yoon, MD¹ ,
Brenda L. Plassman, PhD², and Sharon Fekrat, MD¹ 

Abstract

Purpose: This work assesses the intrasession repeatability of capillary perfusion density (CPD) and capillary flux index (CFI) measurements on peripapillary optical coherence tomography angiography (OCTA) in healthy eyes of older adults. **Methods:** In this cross-sectional study, healthy volunteers aged 50 years or older underwent 4.5×4.5 mm OCTA imaging centered on the optic nerve head using Zeiss Cirrus HD-5000 AngioPlex (Carl Zeiss Meditec). Two consecutive images were acquired in the same eye during a single study session. CPD and CFI were assessed using AngioPlex Software (version 11.0.0.29946) for the radial peripapillary capillary plexus (average over whole scan area) and 4 quadrants (superior, inferior, temporal, and nasal). CPD and CFI repeatability was assessed by intraclass correlation (ICC), mean interocular differences using 2-tailed *t* test, and association with age using generalized estimating equations. **Results:** A total of 150 images were acquired from 75 eyes of 47 patients. For CPD, ICC results ranged from 0.7160 (nasal CPD) to 0.9218 (average CPD). For CFI, ICC results ranged from 0.6167 (temporal CFI) to 0.8976 (inferior CFI). Temporal CFI was significantly different between right and left eyes of the same patient ($P = .03$). CPD and CFI decreased with age in all analyses (average CPD β coefficient -0.00172 , $P < .001$; average CFI β coefficient -0.00278 , $P < .001$). **Conclusions:** Moderate to good repeatability was observed for most peripapillary OCTA metrics; temporal measurements were least repeatable for CPD and CFI. Peripapillary CPD and CFI decrease with age even beyond the fifth decade in healthy older adults.

Keywords

diagnostic test, imaging, instrumentation and devices, OCT, OCT angiography, retina

Introduction

Optical coherence tomography angiography (OCTA) is a noninvasive method of visualizing the retinal microvasculature,¹ giving insight into disease states such as glaucoma,²⁻⁴ diabetic retinopathy,⁵⁻⁷ and recently, neurodegenerative conditions such as Alzheimer disease.⁸⁻¹⁰ However, OCTA image interpretation is highly dependent on scan quality, and image acquisition is susceptible to signal loss and motion artifact.^{11,12} An important focus of OCTA research is whether clinicians can reasonably rely on OCTA measurements and to what extent these parameters reflect clinical change rather than variation inherent to the imaging modality. Studies have shown poor reproducibility of OCTA measurements across different devices, likely due to differences in image resolution, segmentation algorithms, and additional features such as motion tracking across proprietary commercial imaging devices.¹³⁻¹⁵

For accurate clinical interpretation of OCTA results between eyes of the same patient, it is important to understand whether interocular symmetry exists in retinal vascular

parameters. A prior study showed moderate correlation between parafoveal vessel area density between 2 eyes of the same patient.¹⁶ However, another recent study that used a swept-source OCTA device concluded that parafoveal vessel density exhibits poor correlation between eyes of the same individual.¹⁷ It is unclear how well the peripapillary microvasculature is correlated between healthy eyes of the same patient.

The retinal microvasculature exhibits characteristic changes with age, and advanced retinal image analysis may eventually

¹ Department of Ophthalmology, Duke University School of Medicine, Durham, NC, USA

² Department of Psychiatry and Behavioral Sciences, Duke University Medical Center, Durham, NC, USA

Corresponding Author:

Sharon Fekrat, MD, Department of Ophthalmology, Duke University School of Medicine, 2351 Erwin Rd, Durham, NC 27705, USA.

Email: sharon.fekrat@duke.edu

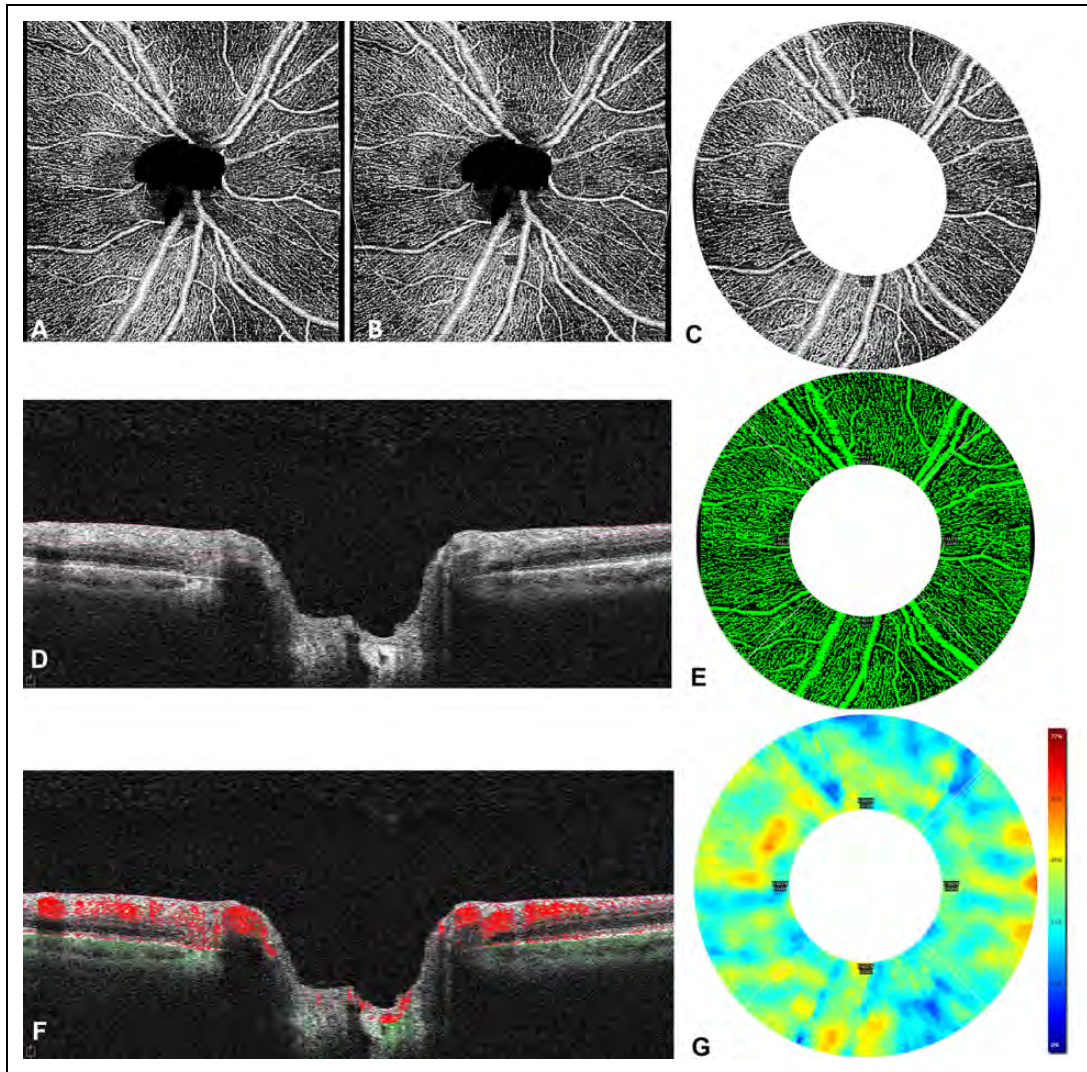


Figure 1. (A) A $4.5 \text{ mm} \times 4.5 \text{ mm}$ peripapillary optical coherence tomography angiography image of the right eye of a study participant is shown. (B) A region of interest, comprising a 2.5-mm wide annulus centered on the optic nerve head with an inner diameter of 2 mm and an outer diameter of 4.5 mm, was overlaid on the image. (C) The areas outside the outer diameter and within the inner diameter, including the optic nerve head, were not included in the analysis. Quantification of the capillary perfusion density and capillary flux index was performed on the 2.5-mm wide annulus. (D) The segmentation boundaries of the radial peripapillary capillary slab extended from the internal limiting membrane to the outer boundary of the retinal nerve fiber layer. (E) A trace map assessing capillary perfusion density was applied within the segmentation boundaries; the perfused vasculature is shown. (F) The flow overlay indicates flow data above the retinal pigment epithelium, and dots indicate flow data below the retinal pigment epithelium. (G) A map of the capillary perfusion density measured as a percentage of the region of interest is shown with its corresponding scale.

be useful for interpreting a person's health status in comparison with chronological age.¹⁸⁻²⁰ In addition to its potential clinical utility, understanding typical peripapillary OCTA changes with increasing age will assist in generating normative OCTA databases for clinical comparison. We hypothesize a slow decline in peripapillary vessel density with increasing age, given the decremental change in cerebral blood flow and retinal blood flow with normal aging.^{21,22}

In this study, we assess the retinal microvasculature using a commercially available OCTA system in a consecutive series of older individuals with healthy eyes to determine the intra-session repeatability of peripapillary OCTA parameters, the

interocular symmetry of these values, and how these values change with increasing age in normal older adults.

Methods

Patient Identification and Data Collection

Healthy individuals aged 50 years or older were enrolled from the Duke Alzheimer's Disease Prevention Registry of nondemented community-dwelling volunteers. Individuals with type 2 diabetes, uncontrolled hypertension, glaucoma, or retinal pathology were excluded. In addition, individuals with

refractive errors of +6.0 diopters (D) or greater or –6.0 D were excluded. All participants underwent testing for corrected Early Treatment Diabetic Retinopathy Study visual acuity the day of enrollment, and individuals with worse than 20/40 visual acuity were excluded from analysis.

All participants underwent imaging by a single experienced photographer with the Zeiss Cirrus HD-5000 Spectral-Domain OCT with AngioPlex OCT Angiography (Carl Zeiss Meditec, software version 11.0.0.29946), which uses motion tracking to reduce motion artifact, has a scan rate of 68 000 A-scans per second, and uses an optical microangiography algorithm for analysis.²³

For each participant, 4.5 × 4.5-mm OCTA images centered on the optic disc were acquired twice in each eye (Figure 1). The scan comprised 350 × 350 A-scans, spaced approximately 12.86 μm apart. Images were manually assessed by trained study staff, and images with poor scan quality (less than 7/10 signal strength index), motion artifact, segmentation artifact, or focal signal loss were excluded. Two metrics of vessel perfusion—capillary perfusion density (CPD) and capillary flux index (CFI)—were calculated using the Zeiss AngioPlex software (version 11.0.0.29946) on en face images that were generated to determine the radial peripapillary capillary plexus, which extended from the internal limiting membrane to the outer boundary of the retinal nerve fiber layer (RNFL) (Figure 1D). A thresholding algorithm was applied to the en face images to create a binary slab, and then a vessel skeleton map was created with vessels linearized into 1-pixel width. CPD and CFI values were generated by the device software, and the numeric data were exported from the machine for statistical analysis.

CPD (reported as a percentage) was defined as the sum of white pixels, which represent the capillaries, in the vessel skeleton map from the linearized OCTA signal divided by the total number of pixels in the region of measurement. It represents the total area of perfused capillary microvasculature per unit area in the region of measurement on the en face images.²⁴

CFI (reported as a unitless ratio) was defined as the total area of the perfused vasculature per unit area in a region of interest on the en face image that was weighted for normalized flow intensity by the brightness of flow signal (Figure 1F) and corrected for dimmer areas on the B-scan.²⁵

Results were generated for CPD and CFI in the 4 quadrants (superior, nasal, inferior, and temporal, which mirror the quadrants used for RNFL quantitative analysis) and an average value over the whole scan area (ie, the CPD for the whole annulus, not divided into quadrants) within a ring-shaped region of interest. This region was a 2.5-mm wide annulus centered on the optic nerve head, which had an inner diameter of 2 mm and an outer diameter of 4.5 mm. The areas outside the outer diameter and within the inner diameter, including the optic nerve head, were not included in the analysis.²⁶ The areas occupied by peripapillary large vessels of more than 32-μm width were not included so that only the capillary density was calculated.

Table 1. Intraclass Correlation and Limits of Agreement for Optical Coherence Tomography Angiography Parameters^a

	Intraclass correlation	95% CI	Limits of agreement
Capillary perfusion density			
Average	0.9218	0.8791-0.9498	–0.020 to 0.018
Superior	0.8440	0.7643-0.8984	–0.038 to 0.035
Nasal	0.7160	0.5855-0.8105	–0.049 to 0.045
Inferior	0.9070	0.8570-0.9402	–0.034 to 0.037
Temporal	0.7371	0.6140-0.8253	–0.054 to 0.051
Capillary flux index			
Average	0.8684	0.7997-0.9417	–0.031 to 0.031
Superior	0.7195	0.5901-0.8129	–0.058 to 0.052
Nasal	0.7751	0.6665-0.8516	–0.055 to 0.055
Inferior	0.8976	0.8429-0.9340	–0.031 to 0.033
Temporal	0.6167	0.4550-0.7392	–0.072 to 0.075

^aAll results are statistically significant with $P < .001$.

Statistical Analysis

Statistical analysis was completed in STATA software version 15.1 (StataCorp). Intrasession repeatability was assessed using a random-effects model for intraclass correlation (ICC) analysis, which accounts for correlations among observations (ie, 2 eyes of the same patient). ICC values can be interpreted as a measure of how tightly clustered measurements within a series of groups are—in the context of this study, it reflects a measurement of the similarity between 2 consecutive measurements in the same eye of the same patient. Higher ICC values indicate greater agreement between the 2 measurements, and lower ICC values indicate worse agreement (ie, greater variation between the 2 measurements). Koo and Li's guidelines for interpreting ICC values were used to report a subjective classification of measurement reliability (less than 0.5 = poor, between 0.5 and 0.75 = moderate, between 0.75 and 0.9 = good, and greater than 0.9 = excellent).²⁷

Bland-Altman analysis generated limits of agreement for average CPD and CFI measurements as well as each optic disc quadrant (superior, nasal, inferior, and temporal). Interocular symmetry was assessed by comparing mean differences in CPD and CFI values between eyes of the same patient using a paired 2-tailed t test. The association of OCTA parameters with age was assessed using generalized estimating equations (GEEs). GEE analysis was used to account for the correlation between 2 eyes of an individual patient. An α of .05 was used to determine statistical significance in all analyses.

Results

A total of 150 images were analyzed from 75 eyes of 47 patients. Twenty-eight images of 19 eyes were excluded from analysis because of the aforementioned image exclusion criteria, including less than 7 of 10 signal strength index, motion artifact, focal signal loss, or segmentation artifact. The mean age of these 47 patients was 68.3 years (range, 61-80 years),

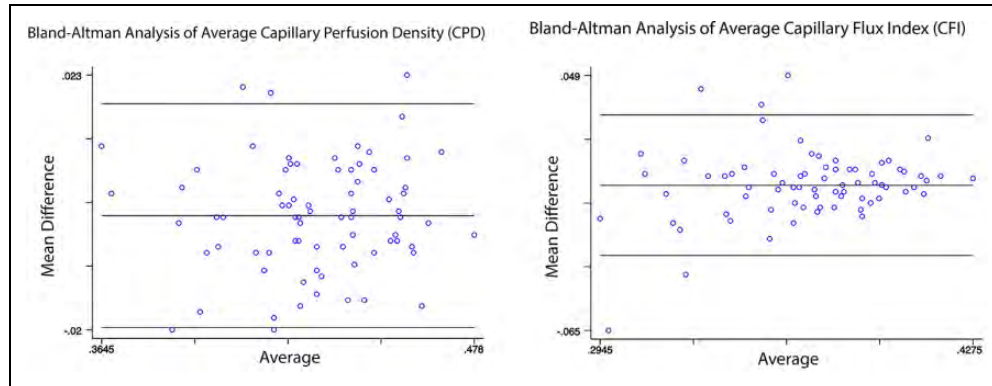


Figure 2. Bland-Altman plot of average (or whole-image) capillary perfusion density (CPD) and capillary flux index (CFI) measurements. Averages of n measurements (2-4) are shown on the x axis, and mean difference between n measurements is shown on the y axis. The middle lines represent the mean differences (CPD = 0.001; CFI = 0.000) and the upper and lower lines represent the limits of agreement (CPD = -0.020, 0.018; CFI = -0.031, 0.031).

and 79% were female. Eighty-four right-eye images (of 42 right eyes) and 66 left-eye images (of 33 left eyes) were acquired. ICC and limits of agreement values for CPD and CFI are reported in Table 1.

We found excellent repeatability for average CPD (ICC = 0.9218) and inferior CPD (ICC = 0.9070). Good repeatability was observed for superior CPD (ICC = 0.8440), average CFI (ICC = 0.8684), nasal CFI (ICC = 0.7751) and inferior CFI (ICC = 0.8976). Moderate repeatability was observed for nasal CPD (ICC = 0.7160), temporal CPD (ICC = 0.7371), superior CFI (ICC = 0.7195), and temporal CFI (ICC = 0.6167). Results of Bland-Altman analysis of average CPD and CFI are shown in Figure 2.

In our analysis of interocular symmetry of OCTA parameters, we included 56 eyes of 28 patients with both eyes imaged. Temporal CFI was found to be significantly different between right and left eyes (right eye 0.364, left eye 0.347, $P = .03$). Peripapillary CPD and CFI values were not significantly different between right and left eyes in all other analyses (all $P > .05$) (Table 2).

Mean CPD for the whole scan was 0.430 (95% CI, 0.424-0.437) in the right eye and 0.431 (95% CI, 0.425-0.437) in the left eye ($P = .69$). Mean CFI for the whole scan was 0.368 (95% CI, 0.362-0.375) in the right eye and 0.366 (95% CI, 0.358-0.374) in the left eye ($P = .63$). Mean CPD values ranged from 0.411 (superior CPD in the right eye) to 0.449 (temporal CPD in the right and left eyes). Mean CFI values ranged from 0.347 (nasal CFI in the left eye and temporal CFI in the left eye) to 0.398 (inferior CFI in the right eye).

Peripapillary CPD and CFI were significantly associated with a decrease in the parameter with an increase in age in the whole scan and all quadrants (all $P < .05$). β coefficients for all variables are reported in Table 3.

In our GEE analysis, β coefficients represent the change in a given parameter for every 1 year of increasing age. For average CPD, the β coefficient for increasing age was -0.00172 ($P < .001$), and for average CFI, the β coefficient for increasing age was -0.00278 ($P < .001$). β coefficients ranged from

Table 2. Average Capillary Perfusion Density and Capillary Flux Index Parameters Grouped by Patient Eye.^a

	Mean (95% CI)	P value
Capillary perfusion density		
Average		
Right	0.430 (0.424-0.437)	.96
Left	0.431 (0.424-0.437)	
Superior		
Right	0.411 (0.402-0.420)	.44
Left	0.416 (0.408-0.424)	
Nasal		
Right	0.416 (0.407-0.425)	.69
Left	0.414 (0.405-0.422)	
Inferior		
Right	0.445 (0.435-0.455)	.99
Left	0.445 (0.434-0.456)	
Temporal		
Right	0.449 (0.439-0.458)	.95
Left	0.449 (0.440-0.458)	
Capillary flux index		
Average		
Right	0.368 (0.362-0.375)	.63
Left	0.366 (0.358-0.374)	
Superior		
Right	0.386 (0.375-0.396)	.91
Left	0.385 (0.376-0.394)	
Nasal		
Right	0.349 (0.337-0.361)	.78
Left	0.347 (0.336-0.357)	
Inferior		
Right	0.398 (0.390-0.406)	.42
Left	0.393 (0.383-0.403)	
Temporal		
Right	0.364 (0.353-0.375)	.03
Left	0.347 (0.335-0.358)	

^aIndividuals with repeated images in both eyes were included in this subanalysis; 112 images of 56 eyes of 28 patients were analyzed.

-0.00129 (nasal CPD) to -0.00317 (temporal CFI). On the whole, β coefficients for CFI were larger than those for CPD, and effect sizes were small but statistically significant.

Table 3. Results of Generalized Estimating Equation Analysis of Optical Coherence Tomography Angiography Parameters Associated With Increasing Age.^a

	β coefficient	95% CI	P
Capillary perfusion density			
Average	-0.00172	-0.00247 to -0.00097	< .001
Superior	-0.00147	-0.00257 to -0.00037	.008
Nasal	-0.00129	-0.00228 to -0.00030	.011
Inferior	-0.00216	-0.00353 to -0.00080	.002
Temporal	-0.00207	-0.00319 to -0.00095	< .001
Capillary flux index			
Average	-0.00278	-0.00364 to -0.00192	< .001
Superior	-0.00266	-0.00374 to -0.00159	< .001
Nasal	-0.00281	-0.00406 to -0.00157	< .001
Inferior	-0.00269	-0.00377 to -0.00161	< .001
Temporal	-0.00317	-0.00423 to -0.00202	< .001

^a β coefficients represent change in a given parameter with each 1 year of increasing age.

Conclusions

We report moderate to good intrasession repeatability for most measurements of peripapillary CPD and CFI using a commercially available OCTA system in healthy eyes of older adults. Peripapillary CPD and CFI results for the whole scan tended to have higher intrasession repeatability, whereas measurements in the optic disc quadrants had lower repeatability. Among the quadrants, inferior measurements had relatively higher repeatability, whereas temporal measurements had relatively lower repeatability. Overall, CPD had higher repeatability than CFI across all measurements. Notably, average CPD had excellent repeatability (ICC = 0.9218).

A number of prior studies have been conducted to specifically assess the repeatability and reproducibility of peripapillary OCTA parameters.^{4,28-31} However, these studies varied regarding imaging device used, image scan size, segmentation algorithm, and study population. In our study, we specifically sought to assess peripapillary OCTA parameter intravisit repeatability (rather than intervisit reproducibility) on the Zeiss AngioPlex OCTA, software version 11, with a dedicated peripapillary 4.5 × 4.5-mm OCTA protocol. Previous studies have used swept-source prototype OCTA²⁸ or Optovue^{4,29-31} imaging systems. These studies have reported ICC values ranging from 0.65 to 0.952. Our study showed excellent repeatability for average CPD and CFI measurements with greater variation in sectoral measurements. We also assessed interocular symmetry and correlation of parameters with age. Thus, our study adds to the growing body of literature supporting the clinical use of peripapillary OCTA.

Sectoral variation in repeatability of peripapillary OCTA parameters may be due to multiple contributing factors, including normal anatomical variation between sectors, patient positioning and fixation during image acquisition, and calculation of CPD and CFI. The nasal and temporal RNFL are thinner, and greater variation has been observed in nasal and temporal RNFL measurements on OCT imaging.³² It is possible that this

normal anatomical variation contributes to greater variation in measured temporal OCTA parameters. Given that OCTA imaging is relatively sensitive to patient positioning and proper fixation, it is possible that the temporal peripapillary area is disproportionately affected by subtle differences in patient positioning. Finally, CPD and CFI rely on assessment of the number of pixels defined as vasculature from a binarized vessel slab generated by the OCTA device. Sectoral measurements have fewer pixels than whole-scan parameters, which may inherently contribute to greater variation given that smaller differences in pixel count could have a larger influence on the final reported parameter.

We found that temporal CFI exhibited significant interocular difference between right and left eyes of the same individual. Although it is possible that this is a false-positive result given that no other parameters (including temporal CPD) were different between eyes of the same patient, it is notable that temporal CFI exhibited the lowest ICC for repeatability (ICC = 0.6167). It is possible that temporal CFI measurements from peripapillary OCTA scans should be approached with greater scrutiny than other measurements.

All peripapillary OCTA parameters significantly decreased with increasing age, although the β coefficients for effect strength were quite small. This finding supports our hypothesis that peripapillary vessel density decreases slowly in healthy eyes of older adults. These findings should be taken into consideration when developing prospectively generated, normative databases of OCTA parameters for healthy, older populations.

An early peripapillary OCTA repeatability study using a Zeiss Cirrus HD-5000 (Carl Zeiss Meditec) prototype in 10 patients showed excellent repeatability and reproducibility.³³ However, we found that repeatability metrics were lower on average, ranging from moderate repeatability to excellent repeatability. We also observed a difference in repeatability by quadrants, with temporal quadrant measurements being less reliable. Another recent study of 30 healthy eyes using a Canon OCT-HS100 angiographic module showed moderate to good repeatability for most OCTA metrics and decreased repeatability in CFI values compared with CPD, which is similar to the results observed in our study.³⁴ It is likely that real-world estimates of repeatability are lower than initially reported by Chen et al,³³ and clinicians should be cautious to interpret small changes in peripapillary CPD or CFI as clinically significant, particularly in sectoral measurements. Further studies assessing the repeatability of these metrics in various states of ocular pathology would be beneficial.

In this study, we did not assess axial length in our patient population, which has been shown to affect OCTA measurements in highly myopic patients.^{35,36} Sampson et al assessed eyes with spherical equivalent between -8 D and +5 D and found that axial lengths in the range 23.29 to 24.33 mm were predicted to correspond to less than 5% change in macular OCTA parameters, suggesting that the impact of axial length is greater in unusually short and long eyes compared with eyes with relatively normal axial lengths.³⁵ We excluded eyes with

refractive errors of +6.0 or greater or -6.0 D to reduce the magnitude of differences due to axial length.

Sampson and colleagues also suggested that because the parafoveal region had a relatively uniform vascular network in healthy eyes, small changes in its boundary from image size correction due to differences in axial length were less likely to induce significant change in overall density.³⁵ The peripapillary region also has a relatively uniform vascular network, and it is likely that image size correction may not induce significant changes. We did not control for optic disc area and recognize that changes in optic disc area may also affect peripapillary measurements on a fixed-size annulus, because for each millimeter increase in axial length, the optic disc area increases by 0.095 mm.³⁷

In our study, we sought to eliminate confounders including interuser variation, so participants underwent imaging by a single experienced photographer to remove this potential confounder in repeatability measurements. Given that multiple photographers may be involved in imaging patients in a typical ophthalmic setting, however, it would be useful to assess variation in measurements among different photographers using the same machine.

The present study has some limitations. We enrolled mostly female patients—this was because of unintended selection bias in recruitment, as our study was broadly advertised to our community registry but mostly female patients chose to enroll. We do not anticipate that repeatability of peripapillary OCTA measurements significantly differs by patient sex; however, this sex difference should be considered when interpreting the results of our study. In addition, we had different numbers of right and left eyes included in the study—this is because we excluded a greater number of left eyes because of motion artifact or poor image quality. This could be in part due to patient fatigue, because we imaged right eyes first, followed by left eyes. However, there were only 9 more right eyes than left eyes, and we included only patients with both eyes imaged in our analysis of interocular symmetry of measurements. Finally, we assessed only individuals without ocular pathology in this study—prior studies with smaller sample sizes have assessed peripapillary OCTA repeatability in disease states using other commercial devices or prototypes. Future research should use Zeiss AngioPlex OCTA in states of ocular pathology.

Future research should aim to determine the repeatability and reproducibility of peripapillary OCTA parameters on newer commercially available devices for comparison, because most published work has been performed using an Optovue imaging system and algorithm. In addition, future studies may assess the repeatability and reproducibility of OCTA measurements in a variety of clinical conditions and settings to ensure that measurement reliability is sufficient for individuals with specific retinal vascular pathologies and in real-world clinical practice.

Authors' Note

This manuscript was presented at the 2020 Association for Research in Vision and Ophthalmology Annual Meeting, which was conducted virtually because of the COVID-19 pandemic.

Ethical Approval

Ethical approval for this cross-sectional study (ClinicalTrials.gov identifier, NCT03233646) was obtained from the Duke Health Institutional Review Board (Pro00082598). This study adhered to the tenets of the Declaration of Helsinki and complied with HIPAA (the Health Insurance Portability and Accountability Act of 1996).

Statement of Informed Consent

Written informed consent was obtained from all participants prior to study enrollment.


Declaration of Conflicting Interests


The author(s) declared no potential conflicts of interest with respect to the research, authorship, and/or publication of this article.


Funding

The author(s) received no financial support for the research, authorship, and/or publication of this article.

ORCID iD

Cason B. Robbins, BS  <https://orcid.org/0000-0001-7909-510X>

Stephen P. Yoon, MD  <https://orcid.org/0000-0002-9974-133X>

Sharon Fekrat, MD  <https://orcid.org/0000-0003-4403-5996>

References

1. Spaide RF, Klancnik JM Jr, Cooney MJ. Retinal vascular layers imaged by fluorescein angiography and optical coherence tomography angiography. *JAMA Ophthalmol.* 2015;133(1):45-50. doi:10.1001/jamaophthalmol.2014.3616
2. Yarmohammadi A, Zangwill LM, Diniz-Filho A, et al. Optical coherence tomography angiography vessel density in healthy, glaucoma suspect, and glaucoma eyes. *Invest Ophthalmol Vis Sci.* 2016;57(9):OCT451-OCT459. doi:10.1167/iovs.15-18944
3. Yarmohammadi A, Zangwill LM, Diniz-Filho A, et al. Relationship between optical coherence tomography angiography vessel density and severity of visual field loss in glaucoma. *Ophthalmology.* 2016;123(12):2498-2508. doi:10.1016/j.ophtha.2016.08.041
4. Liu L, Jia Y, Takusagawa HL, et al. Optical coherence tomography angiography of the peripapillary retina in glaucoma. *JAMA Ophthalmol.* 2015;133(9):1045-1052. doi:10.1001/jamaophthalmol.2015.2225
5. You Q, Freeman WR, Weinreb RN, et al. Reproducibility of vessel density measurement with optical coherence tomography angiography in eyes with and without retinopathy. *Retina.* 2017;37(8):1475-1482. doi:10.1097/IAE.0000000000001407
6. Soares M, Neves C, Marques IP, et al. Comparison of diabetic retinopathy classification using fluorescein angiography and optical coherence tomography angiography. *Br J Ophthalmol.* 2017;101(1):62-68. doi:10.1136/bjophthalmol-2016-309424
7. Pan J, Chen D, Yang X, et al. Characteristics of neovascularization in early stages of proliferative diabetic retinopathy by optical coherence tomography angiography. *Am J Ophthalmol.* 2018;192:146-156. doi:10.1016/j.ajo.2018.05.018
8. Zabel P, Kaluzny JJ, Wilkosc-Debczynska M, et al. Comparison of retinal microvasculature in patients with Alzheimer's disease and primary open-angle glaucoma by optical coherence

- tomography angiography. *Invest Ophthalmol Vis Sci.* 2019; 60(10):3447-3455. doi:10.1167/iovs.19-27028
9. Yoon SP, Grewal DS, Thompson AC, et al. Retinal microvascular and neurodegenerative changes in Alzheimer's disease and mild cognitive impairment compared with control participants. *Ophthalmol Retina.* 2019;3(6):489-499. doi:10.1016/j.oret.2019.02.002
 10. Yoon SP, Thompson AC, Polascik BW, et al. Correlation of OCTA and volumetric MRI in mild cognitive impairment and Alzheimer's disease. *Ophthalmic Surg Lasers Imaging Retina.* 2019;50(11):709-718. doi:10.3928/23258160-20191031-06
 11. Czakó C, István L, Ecsedy M, et al. The effect of image quality on the reliability of OCT angiography measurements in patients with diabetes. *Int J Retina Vitreous.* 2019;5:46. doi:10.1186/s40942-019-0197-4
 12. Holmen IC, Konda MS, Pak JW, et al. Prevalence and severity of artifacts in optical coherence tomographic angiograms. *JAMA Ophthalmol.* 2019;138(2):119-126. doi:10.1001/jamaophthalmol.2019.4971
 13. Arya M, Rebhun CB, Alibhai AY, et al. Parafoveal retinal vessel density assessment by optical coherence tomography angiography in healthy eyes. *Ophthalmic Surg Lasers Imaging Retina.* 2018; 49(10):S5-S17. doi:10.3928/23258160-20180814-02
 14. Lei J, Pei C, Wen C, Abdelfattah NS. Repeatability and reproducibility of quantification of superficial peri-papillary capillaries by four different optical coherence tomography angiography devices. *Sci Rep.* 2018;8(1):17866. doi:10.1038/s41598-018-36279-2
 15. Mihailovic N, Brand C, Lahme L, et al. Repeatability, reproducibility and agreement of foveal avascular zone measurements using three different optical coherence tomography angiography devices. *PLoS One.* 2018;13(10):e0206045. doi:10.1371/journal.pone.0206045
 16. Liu G, Keyal K, Wang F. Interocular symmetry of vascular density and association with central macular thickness of healthy adults by optical coherence tomography angiography. *Sci Rep.* 2017;7(1):16297. doi:10.1038/s41598-017-16675-w
 17. Fang D, Tang FY, Huang H, Cheung CY, Chen H. Repeatability, interocular correlation and agreement of quantitative swept-source optical coherence tomography angiography macular metrics in healthy subjects. *Br J Ophthalmol.* 2019;103(3): 415-420. doi:10.1136/bjophthalmol-2018-311874
 18. Orlov NV, Coletta C, van Asten F, et al. Age-related changes of the retinal microvasculature. *PLoS One.* 2019;14(5):e0215916. doi:10.1371/journal.pone.0215916
 19. Wei Y, Jiang H, Shi Y, et al. Age-related alterations in the retinal microvasculature, microcirculation, and microstructure. *Invest Ophthalmol Vis Sci.* 2017;58(9):3804-3817. doi:10.1167/iovs.17-21460
 20. Scioli MG, Bielli A, Arcuri G, Ferlosio A, Orlandi A. Ageing and microvasculature. *Vasc Cell.* 2014;6:19. doi:10.1186/2045-824X-6-19
 21. Shaw TG, Mortel KF, Meyer JS, Rogers RL, Hardenberg J, Cutaia MM. Cerebral blood flow changes in benign aging and cerebrovascular disease. *Neurology.* 1984;34(7):855-862. doi:10.1212/wnl.34.7.855
 22. Lin Y, Jiang H, Liu Y, et al. Age-related alterations in retinal tissue perfusion and volumetric vessel density. *Invest Ophthalmol Vis Sci.* 2019;60(2):685-693. doi:10.1167/iovs.18-25864
 23. Rosenfeld PJ, Durbin MK, Roisman L, et al. ZEISS Angioplex spectral domain optical coherence tomography angiography: technical aspects. *Dev Ophthalmol.* 2016;56:18-29. doi:10.1159/000442773
 24. Chang R, Chu Z, Burkemper B, et al. Effect of scan size on glaucoma diagnostic performance using OCT angiography en face images of the radial peripapillary capillaries. *J Glaucoma.* 2019;28(5):465-472. doi:10.1097/IJG.0000000000001216
 25. Zeiss *CIRRUS HD-OCT 5000 User Manual.* 2660021169012 Rev. A 2017-12. Carl Zeiss Meditec.
 26. Triolo G, Rabiolo A, Shemonski ND, et al. Optical coherence tomography angiography macular and peripapillary vessel perfusion density in healthy subjects, glaucoma suspects, and glaucoma patients. *Invest Ophthalmol Vis Sci.* 2017;58(13):5713-5722. doi:10.1167/iovs.17-22865
 27. Koo TK, Li MY. A guideline of selecting and reporting intraclass correlation coefficients for reliability research. *J Chiropr Med.* 2016;15(2):155-163. doi:10.1016/j.jcm.2016.02.012
 28. Wang X, Jia Y, Spain R, et al. Optical coherence tomography angiography of optic nerve head and parafovea in multiple sclerosis. *Br J Ophthalmol.* 2014;98(10):1368-1373. doi:10.1136/bjophthalmol-2013-304547
 29. Wang X, Jiang C, Ko T, et al. Correlation between optic disc perfusion and glaucomatous severity in patients with open-angle glaucoma: an optical coherence tomography angiography study. *Graefes Arch Clin Exp Ophthalmol.* 2015;253(9):1557-1564. doi: 10.1007/s00417-015-3095-y
 30. Manalastas PIC, Zangwill LM, Saunders LJ, et al. Reproducibility of optical coherence tomography angiography macular and optic nerve head vascular density in glaucoma and healthy eyes. *J Glaucoma.* 2017;26(10):851-859. doi:10.1097/IJG.0000000000000768
 31. She X, Guo J, Liu X, et al. Reliability of vessel density measurements in the peripapillary retina and correlation with retinal nerve fiber layer thickness in healthy subjects using optical coherence tomography angiography. *Ophthalmologica.* 2018;240(4): 183-190. doi:10.1159/000485957
 32. Blumenthal EZ, Williams JM, Weinreb RN, et al. Reproducibility of nerve fiber layer thickness measurements by use of optical coherence tomography. *Ophthalmology.* 2000;107(12): 2278-2282. doi:10.1016/s0161-6420(96)30410-7
 33. Chen CL, Bojikian KD, Xin C, et al. Repeatability and reproducibility of optic nerve head perfusion measurements using optical coherence tomography angiography. *J Biomed Optics.* 2016; 21(6):065002. doi:10.1117/1.JBO.21.6.065002
 34. Pappelis K, Jansonius NM. Quantification and repeatability of vessel density and flux as assessed by optical coherence tomography angiography. *Trans Vis Sci Technol.* 2019;8(3):3. doi: 10.1167/tvst.8.3.3
 35. Sampson DM, Gong P, An D, et al. Axial length variation impacts on superficial retinal vessel density and foveal avascular zone

- area measurements using optical coherence tomography angiography. *Invest Ophthalmol Vis Sci.* 2017;58(7):3065-3072. doi:10.1167/iovs.17-21551
36. Llanas S, Linderman RE, Chen FK, Carroll J. Assessing the use of incorrectly scaled optical coherence tomography angiography images in peer-reviewed studies: a systematic review. *JAMA Ophthalmol.* 2020;138(1):86-94. doi:10.1001/jamaophthalmol.2019.4821
37. Leung CK, Cheng AC, Chong KK, et al. Optic disc measurements in myopia with optical coherence tomography and confocal scanning laser ophthalmoscopy. *Invest Ophthalmol Vis Sci.* 2007;48(7):3178-3183. doi:10.1167/iovs.06-1315